SABA Publishing

Journal of Fractional Calculus and Nonlinear Systems
jfcns.sabapub.com
ISSN : 2709-9547

J Frac Calc & Nonlinear Sys
(2025)6(1) : 1-28
doi:10.48185/jfcns.v6i1.1449

Mathematical Modeling and Analysis of the Spread of Varicella (Chickenpox) Disease with the Caputo Operator

MUBARAK A. TIJANI [a], KOLADE M. OWOLABI[b,*], MONDAY K. DUROMOLA[c], EDSON PINDZA[d]

[a,b,c] Department of Mathematical Sciences, Federal University of Technology, PMB 704, Akure, Ondo State, Nigeria

[d] Department of Decision Sciences, College of Economic and Management Sciences, University of South Africa (UNISA), Pretoria 0003, South Africa

• *Received: 01 January 2025* • *Accepted: 24 June 2025* • *Published Online: 28 June 2025*

Abstract

In this study, we present a mathematical model for studying the dynamics of varicella disease transmission incorporating Caputo's fractional derivative to account for memory effects in disease spread. The aim of this research is to construct a robust mathematical framework that combines fractional calculus with disease modeling and explore fractional order parameters impacts on diseases propagations. Thus, the significant contribution to knowledge is the improved understanding of infectious diseases? dynamism as influenced by memory effects thus providing profound insights which can be used as cornerstones in developing preventive measures. The technique of this study relies on integration a system of differential equations which are subjected to the Caputo fractional operator. A variety of data sources were used, including existing epidemiological varicella literature for model calibration. We begin by analyzing the existences and uniqueness of the solutions to this model, utilizing the Banach Fixed-point theorem, the linear stability analysis of the model, using Lyapunov Functional approach. The analysis also includes key epidemiological parameters (R_0: basic reproduction number) and dynamic response of the disease-free equilibrium. The effect of the fractional order parameter is investigated through numerical simulations performed by appropriate computational tools especially concerning an infection peak and asymptotic behavior. The results indicate that the varicella transmission dynamics are related to order parameter of fractional order α. The results of this study demonstrated that to better describe epidemiological data, it is essential to introduce fractional order operators within infectious disease models able to represent nonlocal and complex phenomena.

Keywords: Banach fixed-point, Lyapunov function, Fractional derivative, Stability analysis, Numerical results.
2010 MSC: 26A33, 65L05, 65M06, 93C10.

1. Introduction

In recent years, the application of mathematical modeling to the study of infectious diseases has become increasingly advanced, allowing for a more shaded understanding of

*Corresponding author: kmowolabi@futa.edu.ng

disease transmission dynamics. This literature review explores the evolution of mathematical modeling in the context of varicella-zoster virus (VZV) and chickenpox, with a specific focus on the utilization of the Caputo operator to enhance the realism of these models. Varicella, also known as chickenpox, is an infectious disease caused by the varicella-zoster virus (VZV). It primarily affects children, presenting with a characteristic itchy rash, red spots, and blisters that spread across the body. While varicella is generally mild in children, it can lead to severe complications in adults and immunocompromised individuals, such as pneumonia, encephalitis, and bacterial skin infections [9].

Recent research has delved into the pathophysiology of VZV, focusing on its ability to remain dormant in the body and reactivate later as herpes zoster, or shingles, highlighting the long-term implications of the virus [27]. Understanding the mechanisms of VZV latency and reactivation is crucial for developing effective treatments and preventive measures. Studies have shown that the virus can persist in the sensory nerve ganglia and reactivate under certain conditions, leading to shingles, a condition characterized by a painful rash and potential complications like postherpetic neuralgia [17]. This reactivation poses a significant health burden, particularly for older adults and those with weakened immune systems[4].

The global impact of varicella is substantial, especially in regions lacking routine vaccination programs. The World Health Organization (WHO) has reported significant morbidity and economic costs associated with varicella outbreaks. In countries where vaccination programs are well-established, there has been a marked decrease in the incidence and severity of the disease, underscoring the effectiveness of immunization efforts [30]. Despite the success of vaccination programs in many developed countries, disparities in vaccine coverage and access continue to pose challenges globally. In low- and middle-income countries, limited resources and infrastructure often hinder the implementation of widespread vaccination campaigns, leading to persistent outbreaks and high disease burden [12]. Addressing these disparities is essential for achieving global control of varicella [19]. Varicella is highly contagious, spreading primarily through respiratory droplets and direct contact with the fluid from blisters.

The basic reproduction number (R0) for varicella ranges from 8 to 12, reflecting its high transmissibility. While the mortality rate for varicella is relatively low, the disease can lead to severe complications, particularly in high-risk groups such as pregnant women, newborns, and immunocompromised individuals [23]. Complications arising from varicella infections include secondary bacterial infections, pneumonia, encephalitis, and hemorrhagic conditions. These complications can significantly increase the risk of severe outcomes and mortality, particularly among those with compromised immune systems or underlying health conditions [16]. Effective management of varicella cases, especially in high-risk populations, is essential to reduce the associated morbidity and mortality [26]. Vaccination remains the most effective intervention against varicella, significantly reducing the incidence and severity of the disease. The introduction of the varicella vaccine has led to a substantial decline in varicella cases and related complications in countries with robust immunization programs [20]. In addition to vaccination, antiviral treatments such as acyclovir and supportive care play crucial roles in managing severe varicella cases and preventing complications [29]. Public health strategies, including widespread vaccination campaigns and rigorous disease surveillance, are essential for controlling varicella

outbreaks. Effective communication and education about the benefits of vaccination can help increase vaccine uptake and ensure community protection [14]. Targeted vaccination efforts aimed at high-risk populations, such as healthcare workers and immunocompromised individuals, are also vital in reducing the overall burden of the disease [24].

The classical epidemiological models, such as the SIR (Susceptible-Infectious-Recovered) and SEIR (Susceptible-Exposed-Infectious-Recovered) models, have been instrumental in studying the transmission dynamics of varicella. These models utilize ordinary differential equations (ODEs) to describe how individuals move through different disease states over time. By estimating parameters like the basic reproduction number (R0) and infectious period duration, researchers can predict the potential impact of interventions such as vaccination and quarantine on disease spread [15]. These models have been extensively applied to varicella to understand patterns of transmission within populations. They provide insights into how vaccination coverage influences disease incidence and how different control measures can mitigate outbreaks. The classical models serve as foundational tools for epidemiologists, facilitating the evaluation of public health strategies and policies aimed at reducing varicella burden [18].

Fractional models in epidemiology involve derivatives of non-integer order, allowing for the incorporation of memory and hereditary properties into biological systems. The adoption of fractional calculus, particularly using the Caputo operator, has emerged as a promising approach to enhance the fidelity of disease models. These models can capture the long-term memory effects and anomalous diffusion observed in the transmission dynamics of infectious diseases [3]. In the context of varicella, fractional models have been employed to overcome the limitations of classical approaches. By utilizing fractional derivatives, researchers can better simulate the persistence and recurrence behaviors of varicella infections, which are often not fully captured by traditional models [11]. This capability allows for more accurate predictions of disease spread and provides insights into the effectiveness of intervention strategies. Researchers have extended classical epidemiological models to include fractional derivatives, leading to the development of fractional-order differential equations. These extended models provide a more flexible framework for capturing the complexities of biological systems [32]. In the case of varicella, fractional models have been used to explore the impacts of various factors such as vaccination, treatment, and social distancing on the spread of the disease [1]. The inclusion of fractional derivatives allows for the modeling of memory effects, which are crucial for understanding diseases like varicella that can exhibit latency and reactivation. This is particularly relevant for varicella-zoster virus, where the virus can remain dormant and reactivate later in life as shingles.

Fractional models can better capture these dynamics compared to classical models[13]. By using fractional-order differential equations, researchers can more accurately represent the persistence of the virus in a population over time. These models have shown improved performance in fitting epidemiological data and predicting disease outcomes under various scenarios. This flexibility enhances the ability to simulate and analyze the effects of public health interventions [21]. Caputo fractional models offer several advantages over classical models, particularly in their ability to capture memory effects and non-local interactions in disease transmission. These models provide a more accurate description of the dynamics of infectious diseases, especially in cases where the disease exhibits complex

temporal patterns [28]. One significant advantage of Caputo fractional models is their ability to incorporate the history of the disease into the modeling process. This is crucial for diseases like varicella, where past exposure and immunity levels can influence current and future transmission dynamics. By accounting for these historical effects, Caputo models enhance the accuracy of predictions and the effectiveness of intervention strategies [8, 34, 33]. Additionally, Caputo fractional models improve the fit of theoretical models to real-world epidemiological data. This improved fit leads to better predictive power and more reliable forecasts, which are essential for effective public health planning and response. The flexibility of Caputo models allows for the integration of various biological and epidemiological factors, providing a comprehensive framework for disease modeling [31].

This paper will present the task of finding and investigating a mathematical model of the transmission process of varicella in the framework of the Caputo operator. Due to presence of fractional derivatives which are responsible for memory effects and non-uniformity in the distribution of the transmission rates in varicella [3]. The analysis will test the model with regard to the bare reproduction number, stability of the equilibrium points, and effect of parameters in the spread of the disease [10].

2. Mathematical model

The classical model presented in this study builds upon the Almeida, R. et al., [2], Atangana and Baleanu [3] and D'Ovidio, M. et al. [10] framework by incorporating these additional complexities. Specifically, it introduces asymptomatic carrier, partially immune individual, pathogen concentration in the environment. These enhancements provide a more comprehensive and realistic representation of the varicella (chickenpox) transmission dynamics, making the model a valuable tool for public health planning and intervention.

$$
\begin{aligned}
\frac{dS}{dt} &= \Lambda - \beta S\left(\frac{I+A}{N}\right) - (\pi+\mu)S + \delta P,\\
\frac{dE}{dt} &= \beta S\left(\frac{I+A}{N}\right) - (\sigma+\mu)E,\\
\frac{dI}{dt} &= (1-\rho)\sigma E - \gamma_P I - \gamma_R I + \mu I\\
\frac{dA}{dt} &= \rho\sigma E - (\gamma_A+\mu)A, \qquad .\\
\frac{dV}{dt} &= \pi S - \mu V\\
\frac{dP}{dt} &= \gamma_P I - (\delta+\mu)P,\\
\frac{dR}{dt} &= \gamma_R I - \gamma_A A - \mu R,\\
\frac{dW}{dt} &= \phi I - \kappa W.
\end{aligned}
\tag{2.1}
$$

Table 1: Description of the Parameters and values for the Varicella Model

Parameters	**Description**	**Caputo**	**Classical**	**Source**
Λ	Recruitment rate	38 individuals per year	38 individuals per year	[6]
β	Transmission rate	0.8	0.8	[7]
π	Vaccination rate	0.7	0.7	[23]
μ	Natural death rate	0.008 per year	0.08 per year	[30]
σ	Rate at which exposed individuals become infection	0.071 per day	0.071 per day	[5]
γ	Recovery rate	0.056 per day	0.056 per day	[2]
γ_A	Recovery rate from asymptomatic carriers	0.056 per day	0.056 per day	[9]
γ_P	Rate at which infected individuals transition to the partially immune individuals	0.096 per day	0.096 per day	[20]
γ_R	Rate at which infected individuals transition to the recovered individuals	0.096 per day	0.096 per day	[10]
ρ	Fraction of exposed individuals who becomes asymptomatic carriers	0.15	0.12	[12]
δ	Rate at which partially immune individuals lose immunity	0.002 per year	0.02 per year	[22]
ϕ	Rate at which infected individuals contribute to the environmental pathogen concentration	0.05 per year	0.05 per year	[25]
k	Decay rate of the pathogen in the environment	0.2	0.2	[28]
$\propto$	Fractional order	-	$0 < \propto \leqslant 1$	[3]

The Classical Model

1. Asymptomatic Carriers (A): The model assumes presence of asymptotic carriers which are not manifested by symptoms but can further disseminate the disease. This makes it look more real as varicella spreads mainly by asymptomatic transmission.
2. Vaccinated Individuals (V) and Partially Immune(P): Our model consists of compartments for the vaccinated as well partially immune pop jobs which allows us to qualitatively simulate vaccination programmes plus naturally-acquired immunity.
3. Environmental Pathogen Concentration (W): The W input allows the model to consider intermediate variables in transmission from environment, an indirect route that may not operate under all circumstances.

4. Memory Effects with Caputo Operator: Here, by using the Caputo fractional derivative our model is able to account for memory effects which makes it a more realistic representation of disease dynamics over time - incorporating long terms influences such as historical exposures and immunities held.

Satisfying these characteristics will give our model a fuller representation of the dynamics of varicella transmission, which in turn may inform improved public health strategies and interventions. From the system of equations (2.1)
We differentiate the total population
N = S+E+I+A+V+P+R with respect to time t

$$\frac{dN}{dt} = \frac{dS}{dt} + \frac{dE}{dt} + \frac{dI}{dt} + \frac{dA}{dt} + \frac{dV}{dt} + \frac{dP}{dt} + \frac{dR}{dt}. \tag{2.2}$$

Substituting the differential equations in 3.1

$$\begin{aligned} \frac{dN}{dt} = &\left(\Lambda - \beta S\left(\frac{I+A}{N}\right) - (\pi+\mu)\,S + \delta P\right) + \left(\beta S\left(\frac{I+A}{N}\right) - (\sigma+\mu)\,E\right) \\ &+ ((1-\rho)\sigma E - \gamma_P I - \gamma_R I - \mu I) + (\rho\sigma E - (\gamma_A+\mu)A) + (\pi S - \mu V) \\ &+ (\gamma_P I - (\delta+\mu)P) + (\gamma_R I + \gamma_A A - \mu R)\,. \end{aligned} \tag{2.3}$$

By combing similar terms

$$\frac{dN}{dt} = \Lambda - \mu(S + E + I + A + V + P + R) = \Lambda - \mu N. \tag{2.4}$$

Thus, the rate of change of the total population N remains,

$$\frac{dN}{dt} = \Lambda - \mu N.$$

This result indicates that the total population N changes due to the influx of new individuals (Λ) and the natural death rate across all compartments (μN).

3. Analysis of the Caputo Fractional Order Model for SEIAVPRW

The Caputo fractional derivative is a generalization of the classical integer-order derivative to non-integer orders. This approach is useful in modeling systems with memory effects or hereditary properties. Applying the Caputo fractional derivative to the SEIAVPRW model involves replacing the time derivatives in the classical model with Caputo fractional derivatives of order α,where $0 < \alpha \leqslant 1$.

3.1. Caputo Fractional Derivatives

The Caputo Fractional derivatives of a function $f(t)$ of order α is defined as:

$${}^{C}D^{\alpha}_{0,t} f(t) = \frac{1}{\Gamma(1-\alpha)} \int_0^t \frac{f^1(\tau)}{(t-\tau)^{\alpha}}\, d\tau. \tag{3.1}$$

Where Γ is the Gamma function
We define the Caputo Fractional derivative for the classical (SEIAVPRW) model. the state

variables will be denoted as S(t), E(t), I(t), A(t), V(t), P(t), R(t) and W(t) and the fractional order will be α.

$$
\begin{aligned}
{}^{C}D^{\alpha}_{0,t}S(t) &= \frac{1}{\Gamma(1-\alpha)}\int_0^t \frac{\Lambda-\beta S(\tau)\dfrac{I(\tau)+A(\tau}{N}-(\pi+\mu)S(\tau)+\delta P(\tau)}{(t-\tau)^{\alpha}}\,d\tau \\
&= \Lambda-\beta S(t)\frac{I(t)+A(t)}{N}-(\pi+\mu)S(t)+\delta P(t), \\
{}^{C}D^{\alpha}_{0,t}E(t) &= \frac{1}{\Gamma(1-\alpha)}\int_0^t \frac{\beta S(\tau)\frac{I(\tau)+A(\tau)}{N}-(\sigma+\mu)E(\tau)}{(t-\tau)^{\alpha}}\,d\tau \\
&= \beta S(t)\frac{I(t)+A(t)}{N}-(\sigma+\mu)E(t), \\
{}^{C}D^{\alpha}_{0,t}I(t) &= \frac{1}{\Gamma(1-\alpha)}\int_0^t \frac{(1-\rho)\sigma E(\tau)-(\gamma_P(\tau)+\gamma_R(\tau)+\mu)I(\tau)}{(t-\tau)^{\alpha}}\,d\tau \\
&= (1-\rho)\sigma E(t)-(\gamma_P(\tau)+\gamma_R(\tau)+\mu)I(t), \\
{}^{C}D^{\alpha}_{0,t}A(t) &= \frac{1}{\Gamma(1-\alpha)}\int_0^t \frac{\rho\sigma E(\tau)-(\gamma_A+\mu)A(\tau)}{(t-\tau)^{\alpha}}\,d\tau \\
&= \rho\sigma E(t)-(\gamma_A+\mu)A(t), \\
{}^{C}D^{\alpha}_{0,t}V(t) &= \frac{1}{\Gamma(1-\alpha)}\int_0^t \frac{\pi S(\tau)-\mu V(\tau)}{(t-\tau)^{\alpha}}\,d\tau \\
&= \pi S(t)-\mu V(t), \\
{}^{C}D^{\alpha}_{0,t}P(t) &= \frac{1}{\Gamma(1-\alpha)}\int_0^t \frac{\gamma_P I(\tau)-(\delta+\mu)P(\tau)}{(t-\tau)^{\alpha}}\,d\tau \\
&= \gamma_P I(t)-(\delta+\mu)P(t), \\
{}^{C}D^{\alpha}_{0,t}R(t) &= \frac{1}{\Gamma(1-\alpha)}\int_0^t \frac{\gamma_R I(\tau)-\gamma_A A(\tau)-\mu R(\tau)}{(t-\tau)^{\alpha}}\,d\tau \\
&= \gamma_R I(t)-\gamma_A A(t)-\mu R(t), \\
{}^{C}D^{\alpha}_{0,t}W(t) &= \frac{1}{\Gamma(1-\alpha)}\int_0^t \frac{\phi I(\tau)-kW(\tau)}{(t-\tau)^{\alpha}}\,d\tau \\
&= \phi I(t)-kW(t).
\end{aligned}
\qquad . \tag{3.2}
$$

3.2. Positivity and Boundedness

We need to ensure that the solutions for $S(t), E(t), I(t), A(t), V(t), P(t), R(t)$ and $W(t)$ are non-negative and bounded for all $t \geqslant 0$.

Positivity

We show the positivity of the solution, by proving that if the initial conditions

$$S(0), E(0), I(0), A(0), V(0), P(0), R(0), W(0)$$

are non-negative, then $S(t), E(t), I(t), A(t), V(t), P(t), R(t)$ and $W(t)$ remain non-negative for all $t \geqslant 0$.

For the positivity of $S(t)$

$$^{C}D_{0,t}^{\alpha}S(t) = \Lambda - \beta S(t)\frac{I(t)+A(t)}{N} - (\pi+\mu)S(t) + \delta P(t). \tag{3.3}$$

Since $\Lambda \geqslant 0$, β, π, μ, $\delta \geqslant 0$ and $I(t)$, $A(t)$, $P(t) \geqslant 0$, it shows that $S(t)$ will remain non-negative if the initial conditions $S(0) \geqslant 0$.

For the positivity of $E(t)$

$$^{C}D_{0,t}^{\alpha}E(t) = \beta S(t)\frac{I(t)+A(t)}{N} - (\sigma+\mu)E(t). \tag{3.4}$$

Since β, π, $\mu \geqslant 0$ and $S(t)$, $I(t)$, $A(t) \geqslant 0$, it shows that $E(t)$ will remain non-negative if the initial conditions $E(0) \geqslant 0$.

For the positivity of $I(t)$

$$^{C}D_{0,t}^{\alpha}I(t) = (1-\rho)\sigma E(t) - (\gamma_P + \gamma_R + \mu)I(t). \tag{3.5}$$

Since σ, γ, $\mu \geqslant 0$ and $E(t) \geqslant 0$, it shows that $I(t)$ will remain non-negative if the initial conditions $I(0) \geqslant 0$.

For the positivity of $A(t)$

$$^{C}D_{0,t}^{\alpha}A(t) = \rho\sigma E(t) - (\gamma_A + \mu)A(t). \tag{3.6}$$

Since ρ, σ, γ_A, $\mu \geqslant 0$ and $E(t) \geqslant 0$, it shows that $A(t)$ will remain non-negative if the initial conditions $A(0) \geqslant 0$.

For the positivity of $V(t)$

$$^{C}D_{0,t}^{\alpha}V(t) = \pi S(t) - \mu V(t). \tag{3.7}$$

Since π, $\mu \geqslant 0$ and $S(t) \geqslant 0$, it shows that $V(t)$ will remain non-negative if the initial conditions $V(0) \geqslant 0$.

For the positivity of $P(t)$

$$^{C}D_{0,t}^{\alpha}P(t) = \gamma_P I(t) - (\delta+\mu)P(t). \tag{3.8}$$

Since γ_R, δ, $\mu \geqslant 0$ and $I(t) \geqslant 0$, it shows that $P(t)$ will remain non-negative if the initial conditions $P(0) \geqslant 0$.

For the positivity of $R(t)$

$$^{C}D_{0,t}^{\alpha}R(t) = \gamma I(t) - \gamma_A A(t) - \mu R(t). \tag{3.9}$$

Since γ, γ_A, $\mu \geqslant 0$ and $I(t) \geqslant 0$, it shows that $R(t)$ will remain non-negative if the initial conditions $R(0) \geqslant 0$.

For the positivity of $W(t)$

$$^{C}D_{0,t}^{\alpha}W(t) = \phi I(t) - kW(t). \tag{3.10}$$

Since ϕ, $k \geqslant 0$ and $I(t) \geqslant 0$, it shows that $W(t)$ will remain non-negative if the initial conditions $W(0) \geqslant 0$.

Boundedness

To prove the boundedness, we show that there exist constants $S_M, E_M, I_M, A_M, V_M, P_M, R_M, W_M$ such that

$$\begin{aligned}\lim_{t\longrightarrow\infty} \sup S(t) \leqslant S_M\ ,\ \lim_{t\longrightarrow\infty} \sup E(t) \leqslant E_M\ ,\ \lim_{t\longrightarrow\infty} \sup I(t) \leqslant I_M\ ,\ \lim_{t\longrightarrow\infty} \sup A(t)\\ \leqslant A_M\ ,\ \lim_{t\longrightarrow\infty} \sup V(t) \leqslant V_M\ ,\ \lim_{t\longrightarrow\infty} \sup P(t) \leqslant P_M\ ,\ \lim_{t\longrightarrow\infty} \sup R(t).\\ \leqslant R_M\ ,\ \lim_{t\longrightarrow\infty} \sup W(t) \leqslant W_M\end{aligned} \tag{3.11}$$

Consider the total population N(t)=S(t)+E(t)+I(t)+A(t)+V(t)+P(t)+R(t)+W(t).
Summing the equation gives

$$^{C}D_t^{\alpha} N(t) = \Lambda - \mu N(t) - kW(t)$$

Since $W(t) \geqslant 0$ and $\mu > 0$, the equation simplifies to

$$^{C}D_t^{\alpha} N(t) \leqslant \Lambda - \mu N(t)$$

This is a linear fractional differential equation. Its solution is given by

$$N(t) \leqslant \frac{\Lambda}{\mu}$$

Hence, the total population N(t) is bounded by $\frac{\Lambda}{\mu}$.
Now, each compartment is a function of the total population and since N(t) is bounded, each compartment is also bounded. Specifically, there exist constant

$$S_M, E_M, I_M, A_M, V_M, P_M, R_M, W_M$$

such that:

$$S(t) \leqslant S_M, E(t) \leqslant E_M, I(t) \leqslant I_M, A(t) \leqslant A_M, V(t) \leqslant V_M,\ P(t) \leqslant P_M,\ R(t) \leqslant R_M,\ W(t) \leqslant W_M$$

Where $S_M, E_M, I_M, A_M, V_M, P_M, R_M, W_M$ are derived from the maximum possible values that each compartment can attain, considering the bounds on N(t).

3.3. Existence and Uniqueness

To prove the existence and uniqueness of solutions for the Caputo fractional model, we need to use results from the theory of fractional equations. We will employ the Banach fixed-point theorem (also known as the contraction mapping theorem), which is a common tool for establishing the existence and uniqueness of solutions to fractional differential equations.

Lipschitz condition

The Lipschitz condition ensures that the function f(t,y) does not change too rapidly and that the system is well-behaved. Specifically, we need to show:

$$\left\|f(t,y_{1)}-f(t,y_2)\right\| \leqslant L\left\|y_1-y_2\right\|. \tag{3.12}$$

For some constant L and for all y_1, y_2 in the domain of interest.
For the first equation

$$\begin{aligned}\left|f(t,y_{1)}-f(t,y_2)\right| &= \left|(\Lambda-\beta S_1\left(\frac{I_1+A_1}{N}\right)-(\pi+\mu)\,S_1+\delta P_1)-(\Lambda-\beta S_2\left(\frac{I_2+A_2}{N}\right)-(\pi+\mu)\,S_2+\delta P_2)\right| \\ &= \left|\beta\left(S_1\frac{I_1+A_1}{N}-S_2\frac{I_2+A_2}{N}\right)-\pi(S_1-S_2)-\mu(S_1-S_2)+\delta(P_1-P_2)\right|.\end{aligned} \tag{3.13}$$

Using properties of absolute values and the fact that the coefficient β, π, μ, δ are constant, we can bound the expression:

$$\begin{aligned}\left|f(t,y_{1)}-f(t,y_2)\right| &\leqslant \beta\left|S_1\frac{I_1+A_1}{N}-S_2\frac{I_2+A_2}{N}\right|+\pi\left|S_1-S_2\right|+\mu\left|S_1-S_2\right|+\delta\left|P_1-P_2\right| \\ &\leqslant \beta\left(|S_1|\left|\frac{I_1+A_1}{N}-\frac{I_2+A_2}{N}\right|+\left|\frac{S_2+S_2}{N}\right||I_2-A_2|\right)+(\pi+\mu)\left|S_1-S_2\right|+\delta\left|P_1-P_2\right|\end{aligned}. \tag{3.14}$$

Since S, I, A, P are bounded by N, we can factor out $\|y_1-y_2\|$:

$$\left|f(t,y_{1)}-f(t,y_2)\right| \leqslant L\left\|y_1-y_2\right\|. \tag{3.15}$$

Where L is a constant that depends on the parameters and the bounds of the state variables.

Banach's fixed-point theorem

Banach's fixed-point theorem (also known as the contraction mapping theorem) is a fundamental result in fixed-point theory. It provides conditions under which a function (or operator) will have a unique fixed point. A fixed point of a function T is a point y such that $T(y) = y$.
Let (X,d) be a non-empty complete metric space with a contraction mapping T: X→X. Then T has a unique fixed point y∈X. Additionally, for any initial point y_0∈X, the sequence defined by y_{n+1}=T($y_{n)}$ converges to the fixed-point y.
A contraction mapping is a function T that brings points closer together, i.e, there exist a constant o⩽k < 1 such that for all y_1, y_2∈X.

$$d(T(y_1),T(y_2))\leqslant k.d(y_1, y_2). \tag{3.16}$$

For the Caputo fractional derivative, the integral form of the differential equation is

$$^{C}D^{\alpha}_{0,t}y\,(t) = f(t, y(t))$$

can be transformed into:

$$y(t) = y(0) + \frac{1}{\Gamma(\propto)} \int_0^t (t-\tau)^{\alpha-1} f(\tau, y(\tau)) d\tau. \tag{3.17}$$

This form allows us to define an operator T acting on a suitable function space.
For our system, let's write the integral form of each equation.
For instance, for S(t):

$$S(t) = S(0) + \frac{1}{\Gamma(\propto)} \int_0^t (t-\tau)^{\alpha-1} (\Lambda - \beta S(\tau) \frac{I(\tau) + A(\tau)}{N} - (\pi+\mu) S(\tau) + \delta P(\tau)) d\tau. \tag{3.18}$$

Similarly, we write the integral forms for E(t), I(t), A(t), V(t), P(t), R(t) and W(t).
We need to show that our operator T is a contraction mapping. This involves demonstrating that there exists a constant k< 1 such that for all $y_1(t)$ and y_2,

$$\|T(y_1) - T(y_2)\| \leqslant k \|y_1 - y_2\|. \tag{3.19}$$

Consider the operator T defined by

$$T(y)(t) = y(0) + \frac{1}{\Gamma(\propto)} \int_0^t (t-\tau)^{\alpha-1} f(\tau, y(\tau)) d\tau. \tag{3.20}$$

For any two functions $y_1(t)$ and $y_2(t)$,

$$T(y_1)(t) - T(y_2)(t) = \frac{1}{\Gamma(\propto)} \int_0^t (t-\tau)^{\alpha-1} (f(\tau, y_1(\tau) - f(\tau, y_2(\tau))) d\tau. \tag{3.21}$$

Using the fact that f satisfies the Lipschitz condition,

$$|f(\tau, y_1(\tau)) - f(\tau, y_2(\tau))| \leqslant L |y_1(\tau) - y_2(\tau)|. \tag{3.22}$$

$$|T(y_1)(t) - T(y_2)(t)| \leqslant \frac{L}{\Gamma(\propto)} \int_0^t (t-\tau)^{\alpha-1} |y_1(\tau) - y_2(\tau)| \, d\tau$$

This shows that T brings $y_1(t)$ and $y_2(t)$ closer together, proving T is a contraction mapping with a contraction constant $k = \frac{L}{\Gamma(\propto)}$.
By Banach's fixed-point theorem, since T is a contraction mapping on a complete metric space, T has a unique fixed point. This fixed point corresponds to the unique solution of our integral equation.

3.4. Disease-free equilibrium (DFE) of the Caputo fractional model

The DFE corresponds to the state where there are no infections in the population. Thus, we set E(t)=0, I(t)=0, A(t)=0, P(t)=0. R(t)=0 and W(t)=0. We denote the equilibrium values as S^*, V^*.
At the DFE, the derivatives with respect to time should be zero. Therefore, we set the left-hand side of each equation to zero and solve for S^*, V^*.

$$\begin{aligned} 0 &= \Lambda - \pi S^* - \mu S^* + \delta P^* \\ 0 &= \pi S^* - \mu V^* \\ 0 &= \gamma_P I^* - (\delta+\mu) P^* \\ 0 &= \gamma_R I^* - \gamma_A - \mu R^* \\ 0 &= \phi I^* - k W^* \end{aligned} \quad . \tag{3.23}$$

Since $I^*=0$, $A^*=0$, $P^*=0$, $R^*=0$ and $W^*=0$, we have the simplified system:

$$\begin{aligned} 0 &= \Lambda - \pi S^* - \mu S^* \\ 0 &= \pi S^* - \mu V^* \end{aligned}. \tag{3.24}$$

From the first equation,

$$0 = \Lambda - \pi S^* - \mu S^* \Longrightarrow V^* = \frac{\pi S^*}{\mu} = \frac{\pi \Lambda}{\mu(\pi+\mu)}$$

The disease-free equilibrium (DFE) for the Caputo fractional model is given by

$$(S^*, E^*, I^*, A^*, V^*, P^*, R^*, W^*) = (\frac{\Lambda}{\pi+\mu}, 0, 0, 0, \frac{\pi\Lambda}{\mu\,(\pi+\mu)}, 0, 0, 0). \tag{3.25}$$

This solution indicates that, in the absence of infection, the population will stabilize with only susceptible and vaccinated individuals, with no exposed, infected or recovered individuals.

3.5. The basic reproduction number R_0

This is a critical threshold parameter that determines whether an infectious disease can invade and spread through a population. For the Caputo Fractional model, we use the Next-Generation matrix approach to derive R_0.
We focus on the infected compartments E and I and linearize the system around the disease-free equilibrium (DFE).

Next-generation matrix

The Next-Generation matrix, FV^{-1} is derived from the matrices F (new infection terms) and V (transition terms) evaluated at the DFE.
At the DFE, $S^*=\frac{\Lambda}{\pi+\mu}$, $V^*=\frac{\pi\Lambda}{\mu(\pi+\mu)}$
The new infection term (F) is given by

$$F = \begin{pmatrix} \beta S^* \frac{I}{N} & \beta S^* \frac{A}{N} & 0 \\ 0 & 0 & 0 \\ 0 & 0 & 0 \end{pmatrix}. \tag{3.26}$$

Substituting $S^*=\frac{\Lambda}{\pi+\mu}$

$$F = \begin{pmatrix} \beta(\frac{\Lambda}{\pi+\mu}) & \beta(\frac{\Lambda}{\pi+\mu}) & 0 \\ 0 & 0 & 0 \\ 0 & 0 & 0 \end{pmatrix}. \tag{3.27}$$

And the transition term (V) given by:

$$V = \begin{pmatrix} \sigma+\mu & 0 & 0 \\ -\sigma & \gamma+ & 0 \\ -\rho\sigma & 0 & \gamma_A+\mu \end{pmatrix}. \tag{3.28}$$

To compute V^{-1}, we need the inverse of V

$$V^{-1}=\begin{pmatrix} \frac{1}{\sigma+\mu} & 0 & 0 \\ \frac{\sigma}{(\gamma+\mu)(\sigma+\mu)} & \frac{1}{\gamma+\mu} & 0 \\ \frac{\rho\sigma}{(\gamma_A+\mu)(\gamma+\mu)(\sigma+\mu)} & 0 & \frac{1}{\gamma_A+\mu} \end{pmatrix}. \tag{3.29}$$

$$FV^{-1}=\begin{pmatrix} \beta(\frac{\Lambda}{\pi+\mu}) & \beta(\frac{\Lambda}{\pi+\mu}) & 0 \\ 0 & 0 & 0 \\ 0 & 0 & 0 \end{pmatrix} \begin{pmatrix} \frac{1}{\sigma+\mu} & 0 & 0 \\ \frac{\sigma}{(\gamma+\mu)(\sigma+\mu)} & \frac{1}{\gamma+\mu} & 0 \\ \frac{\rho\sigma}{(\gamma_A+\mu)(\gamma+\mu)(\sigma+\mu)} & 0 & \frac{1}{\gamma_A+\mu} \end{pmatrix}. \tag{3.30}$$

$$= \begin{pmatrix} \beta(\frac{\Lambda}{\pi+\mu})(\frac{1}{\sigma+\mu}+\frac{\sigma}{(\gamma+\mu)(\sigma+\mu)}) & \beta(\frac{\Lambda}{\pi+\mu})(\frac{1}{\gamma+\mu}) & 0 \\ 0 & 0 & 0 \\ 0 & 0 & 0 \end{pmatrix}. \tag{3.31}$$

The dominant eigenvalue of the matrix FV^{-1} gives the basic reproduction number R_0. We need the dominant eigenvalue of the first row, first column:

$$R_0=\beta\left(\frac{\Lambda}{\pi+\mu}\right)\left(\frac{1}{\sigma+\mu}+\frac{\sigma}{(\gamma+\mu)(\sigma+\mu)}\right). \tag{3.32}$$

This is the basic reproduction number for the Caputo Fractional SEIAPRW model.

3.6. Global stability of the disease-free equilibrium (DFE)

We use a Lyapunov functional approach, which is effective for fractional-order systems. To establish global stability, we construct a Lyapunov functional V that satisfies the following conditions:

1. V is positive definite;
2. The fractional derivative of V along the solutions of the system is negative definite.

We propose a Lyapunov functional for the Caputo fractional model

$$V(t)=E(t)+I(t)+A(t). \tag{3.33}$$

The Caputo fractional derivative of V(t) is

$${}^{C}D^{\alpha}_{0,t}V(t)={}^{C}D^{\alpha}_{0,t}E(t)+{}^{C}D^{\alpha}_{0,t}I(t)+{}^{C}D^{\alpha}_{0,t}A(t). \tag{3.34}$$

Substitute the model equations:

$$\begin{aligned} {}^{C}D^{\alpha}_{0,t}E(t)&=\beta S(t)\frac{I(t)+A(t)}{N}-(\sigma+\mu) \\ {}^{C}D^{\alpha}_{0,t}I(t)&=(1-\rho)\sigma E(t)-(\gamma_P+\gamma_R+\mu)I(t)\cdot \\ {}^{C}D^{\alpha}_{0,t}A(t)&=\rho\sigma E(t)-(\gamma_A+\mu)I(t) \end{aligned} \tag{3.35}$$

Then,

$$
\begin{aligned}
&{}^{C}D^{\propto}_{0,t}V(t) = {}^{C}D^{\propto}_{0,t}E(t) + {}^{C}D^{\propto}_{0,t}I(t) + {}^{C}D^{\propto}_{0,t}A(t) \\
&= \beta S(t)\frac{I(t)+A(t)}{N} - (\sigma+\mu)E + (1-\rho)\sigma E(t) - (\gamma_P+\gamma_R+\mu)I(t) + \rho\sigma E(t) - (\gamma_A+\mu)I(t). \\
&= \beta S(t)\frac{I(t)+A(t)}{N} + (\sigma-\sigma-\mu+\rho\sigma)E(t) - (\gamma_P+\gamma_R+\mu)I(t) - (\gamma_A+\mu)A(t)
\end{aligned}
\tag{3.36}
$$

For the DFE to be globally stable, the total derivative ${}^{C}D^{\alpha}_{0,t}V(t)$ must be non-positive. This can be ensured if the decay terms dominate the infection and growth terms. We particularly need to consider the basic reproduction number R_0:

$$
R_0 = \frac{\beta S^*}{\gamma+\mu}. \tag{3.37}
$$

When $R_0 \leqslant 1$, the infection terms cannot sustain the spread of the disease, leading to a natural decline in I(t) and A(t). Specifically, if $\beta S(t)\frac{I(t)+A(t)}{N}$ (Infection terms) is small enough and $(\mu+\rho\sigma)E(t)$ (transition/growth terms) is balanced or outweighed by $-(\gamma+\mu)I(t)$ and $-(\gamma_A+\mu)A(t)$ (decay terms), then the overall derivative ${}^{C}D^{\alpha}_{0,t}V(t) \leqslant 0$.

3.7. Local stability of the disease-free equilibrium state

We use the method of Linearization and the fractional Jacobian matrix.
To determine the local stability, we evaluate the Jacobian matrix at the DFE. Let's find the Jacobian matrix J for the system at the DFE, the Jacobian matrix is given by the partial derivatives of the right-hand sides of the system of equations with respect to S,E,I,A,V,P,R,W.

$$
J = \begin{pmatrix}
\frac{\partial({}^{c}D^{\propto}_{t}S)}{\partial S} & \frac{\partial({}^{c}D^{\propto}_{t}S)}{\partial E} & \frac{\partial({}^{c}D^{\propto}_{t}S)}{\partial I} & \frac{\partial({}^{c}D^{\propto}_{t}S)}{\partial A} & \frac{\partial({}^{c}D^{\propto}_{t}S)}{\partial V} & \frac{\partial({}^{c}D^{\propto}_{t}S)}{\partial P} & \frac{\partial({}^{c}D^{\propto}_{t}S)}{\partial R} & \frac{\partial({}^{c}D^{\propto}_{t}S)}{\partial W} \\
\frac{\partial({}^{c}D^{\propto}_{t}E)}{\partial S} & \frac{\partial({}^{c}D^{\propto}_{t}E)}{\partial E} & \frac{\partial({}^{c}D^{\propto}_{t}E)}{\partial I} & \frac{\partial({}^{c}D^{\propto}_{t}E)}{\partial A} & \frac{\partial({}^{c}D^{\propto}_{t}E)}{\partial V} & \frac{\partial({}^{c}D^{\propto}_{t}E)}{\partial P} & \frac{\partial({}^{c}D^{\propto}_{t}E)}{\partial R} & \frac{\partial({}^{c}D^{\propto}_{t}E)}{\partial W} \\
\frac{\partial({}^{c}D^{\propto}_{t}I)}{\partial S} & \frac{\partial({}^{c}D^{\propto}_{t}I)}{\partial E} & \frac{\partial({}^{c}D^{\propto}_{t}I)}{\partial I} & \frac{\partial({}^{c}D^{\propto}_{t}I)}{\partial A} & \frac{\partial({}^{c}D^{\propto}_{t}I)}{\partial V} & \frac{\partial({}^{c}D^{\propto}_{t}I)}{\partial P} & \frac{\partial({}^{c}D^{\propto}_{t}I)}{\partial R} & \frac{\partial({}^{c}D^{\propto}_{t}I)}{\partial W} \\
\frac{\partial({}^{c}D^{\propto}_{t}A)}{\partial S} & \frac{\partial({}^{c}D^{\propto}_{t}A)}{\partial E} & \frac{\partial({}^{c}D^{\propto}_{t}I)}{\partial A} & \frac{\partial({}^{c}D^{\propto}_{t}A)}{\partial A} & \frac{\partial({}^{c}D^{\propto}_{t}A)}{\partial V} & \frac{\partial({}^{c}D^{\propto}_{t}A)}{\partial P} & \frac{\partial({}^{c}D^{\propto}_{t}A)}{\partial R} & \frac{\partial({}^{c}D^{\propto}_{t}A)}{\partial W} \\
\frac{\partial({}^{c}D^{\propto}_{t}V)}{\partial S} & \frac{\partial({}^{c}D^{\propto}_{t}V)}{\partial E} & \frac{\partial({}^{c}D^{\propto}_{t}I)}{\partial A} & \frac{\partial({}^{c}D^{\propto}_{t}V)}{\partial A} & \frac{\partial({}^{c}D^{\propto}_{t}V)}{\partial V} & \frac{\partial({}^{c}D^{\propto}_{t}V)}{\partial P} & \frac{\partial({}^{c}D^{\propto}_{t}V)}{\partial R} & \frac{\partial({}^{c}D^{\propto}_{t}V)}{\partial W} \\
\frac{\partial({}^{c}D^{\propto}_{t}P)}{\partial S} & \frac{\partial({}^{c}D^{\propto}_{t}P)}{\partial E} & \frac{\partial({}^{c}D^{\propto}_{t}I)}{\partial A} & \frac{\partial({}^{c}D^{\propto}_{t}P)}{\partial A} & \frac{\partial({}^{c}D^{\propto}_{t}P)}{\partial V} & \frac{\partial({}^{c}D^{\propto}_{t}P)}{\partial P} & \frac{\partial({}^{c}D^{\propto}_{t}P)}{\partial R} & \frac{\partial({}^{c}D^{\propto}_{t}P)}{\partial W} \\
\frac{\partial({}^{c}D^{\propto}_{t}R)}{\partial S} & \frac{\partial({}^{c}D^{\propto}_{t}R)}{\partial E} & \frac{\partial({}^{c}D^{\propto}_{t}I)}{\partial I} & \frac{\partial({}^{c}D^{\propto}_{t}R)}{\partial A} & \frac{\partial({}^{c}D^{\propto}_{t}R)}{\partial V} & \frac{\partial({}^{c}D^{\propto}_{t}R)}{\partial P} & \frac{\partial({}^{c}D^{\propto}_{t}R)}{\partial R} & \frac{\partial({}^{c}D^{\propto}_{t}R)}{\partial W} \\
\frac{\partial({}^{c}D^{\propto}_{t}W)}{\partial S} & \frac{\partial({}^{c}D^{\propto}_{t}W)}{\partial E} & \frac{\partial({}^{c}D^{\propto}_{t}I)}{\partial I} & \frac{\partial({}^{c}D^{\propto}_{t}W)}{\partial A} & \frac{\partial({}^{c}D^{\propto}_{t}W)}{\partial V} & \frac{\partial({}^{c}D^{\propto}_{t}W)}{\partial P} & \frac{\partial({}^{c}D^{\propto}_{t}W)}{\partial R} & \frac{\partial({}^{c}D^{\propto}_{t}W)}{\partial W}
\end{pmatrix}. \tag{3.38}
$$

evaluating the partial derivatives at the DFE,

$$\begin{pmatrix} -(\pi+\mu) & 0 & -\frac{\beta\Lambda}{N(\pi+\mu)} & -\frac{\beta\Lambda}{N(\pi+\mu)} & 0 & \delta & 0 & 0 \\ 0 & -(\sigma+\mu) & \frac{\beta\Lambda}{N(\pi+\mu)} & \frac{\beta\Lambda}{N(\pi+\mu)} & 0 & 0 & 0 & 0 \\ 0 & \sigma & -(\gamma_P+\gamma_R+\mu) & 0 & 0 & 0 & 0 & 0 \\ 0 & \rho\sigma & 0 & -(\gamma_A+\mu) & 0 & 0 & 0 & 0 \\ \pi & 0 & 0 & 0 & -\mu & 0 & 0 & 0 \\ 0 & 0 & \gamma & 0 & 0 & -(\gamma+\mu) & 0 & 0 \\ 0 & 0 & \gamma & \gamma_A & 0 & 0 & -\mu & 0 \\ 0 & 0 & \phi & 0 & 0 & 0 & 0 & -\kappa \end{pmatrix}. \tag{3.39}$$

The local stability of the DFE depends on the eigenvalues of the Jacobian matrix. If all eigenvalues have negative real parts, the DFE is locally asymptotically stable.
The characteristics equation is obtained by solving $det\,(J-\lambda I)=0$.
Where λ is an eigenvalue and I is the identity matrix
Solving the determinant

$$\begin{vmatrix} -(\pi+\mu)-\lambda & 0 & -\frac{\beta\Lambda}{N(\pi+\mu)} & -\frac{\beta\Lambda}{N(\pi+\mu)} & 0 & \delta & 0 & 0 \\ 0 & -(\sigma+\mu)-\lambda & \frac{\beta\Lambda}{N(\pi+\mu)} & \frac{\beta\Lambda}{N(\pi+\mu)} & 0 & 0 & 0 & 0 \\ 0 & \sigma & -(\gamma_P+\gamma_R+\mu)-\lambda & 0 & 0 & 0 & 0 & 0 \\ 0 & \rho\sigma & 0 & -(\gamma_A+\mu)-\lambda & 0 & 0 & 0 & 0 \\ \pi & 0 & 0 & 0 & -\mu-\lambda & 0 & 0 & 0 \\ 0 & 0 & \gamma & 0 & 0 & -(\gamma+\mu)-\lambda & 0 & 0 \\ 0 & 0 & \gamma & \gamma_A & 0 & 0 & -\mu-\lambda & 0 \\ 0 & 0 & \phi & 0 & 0 & 0 & 0 & -\kappa-\lambda \end{vmatrix}. \tag{3.40}$$

The eigenvalues are:

$$\lambda_1=-(\pi+\mu),\ \lambda_2=-(\sigma+\mu),\ \lambda_3=-(\gamma+\mu),\ \lambda_4=-(\gamma_A+\mu),\ \lambda_5=-\mu,\ \lambda_6=-(\delta+\mu),$$
$$\lambda_7=-\mu,\ \lambda_8=-k. \tag{3.41}$$

All eigenvalues have negative real parts, ensuring the local stability of the disease-free equilibrium.
Since all the eigenvalues have negative real parts, the DFE of the Caputo fractional model is locally asymptotically stable. This means small perturbations around the DFE will decay over time, leading the system back to the DFE, indicating that the disease will die out in the long run if the initial infection is small.

Backward bifurcation in the varicella transmission model

We study the existence of multiple equilibria when $R_0 < 1$ to establish the occurrence of backward bifurcation. In particular, we compute the equilibrium equations to identifying conditions under which a positive endemic equilibrium is present.

Endemic equilibrium

In equilibrium, all the derivatives of state variables are equal to zero. For simplicity, we consider the force of infection term:

$$\lambda = \beta \frac{I + A}{N}. \tag{3.42}$$

Substituting into (54) for I and A, we obtain:

$$I^* = \frac{(1-\rho)\sigma E^*}{\gamma_P + \gamma_R + \mu}, \; A^* = \frac{\rho\sigma E^*}{\gamma_A + \mu}. \tag{3.43}$$

Using these expressions, the equations for E^* becomes:

$$E^* = \frac{\beta S^*(I^* + A^*)}{\sigma + \mu}. \tag{3.44}$$

Substituting I^* and A^* into (56) yields a quadratic equation for E^*:

$$aE^{*2} + bE^* + c = 0. \tag{3.45}$$

Where a, b and c are parameters function

Condition for backward bifurcation

Backward bifurcation occurs if the quadratic equation has two positive roots for E^* when $R_0 < 1$. This requires:

1. The discriminant $\Delta = b^2 - 4ac > 0$,
2. $c < 0$, means one root is positive. These conditions rely on certain parameter values, especially those associated with vaccine rate (π), recovery rate (γ) and transmission rate (β)

4. Numerical method

For our SEIAVPRW model, we need to discretize the Caputo dfractional derivatives. One effective method is using the Grünwald-Letnikov approximation, which can be adapted for a numerical integration scheme like the Adams-Bashforth method. Here, we integrate the Caputo derivative into our numerical scheme.

For a function f(t), the Caputo dfractional derivative of order α at the n-th time step can be approximated as:

$${}^{C}D^{\alpha}_{0,t} y(t) \approx \frac{1}{h^{\alpha}} \sum_{k=0}^{n} w_k y(t_{n-k}). \tag{4.1}$$

where w_k are the Grünwald-Letnikov weights defined as

$$w_k = (-1)^k \binom{\alpha}{k}$$

and $\binom{\alpha}{k}$ is the generalized binomial coefficient.

The Adams-Bashforth method approximates the solution at t_{n+2} based on the previous two steps:

$$y_{n+2}=y_{n+1}+\frac{3}{2}hf\left(t_{n+1},y_{n+1}\right)-\frac{1}{2}hf\left(t_n,y_n\right). \tag{4.2}$$

To combine this with the Caputo derivative, we modify the Adams-Bashforth scheme to incorporate the dfractional terms. The modified scheme is as follows:

$$y_{n+2}=y_{n+1}+\frac{3}{2}h{}^{C}D_{0,t}^{\alpha}f\left(t_{n+1},y_{n+1}\right)-\frac{1}{2}h{}^{C}D_{0,t}^{\alpha}f\left(t_n,y_n\right). \tag{4.3}$$

To start the process, we need initial conditions y_0 and y_1, which can be computed using an Euler method:

$$y_1 = y_0 + hf(t_0, y_0). \tag{4.4}$$

To applying the scheme to SEIAVPRW model, we define f(t,y) for each state variable and apply the modified Adams-Bashforth scheme.

For example, fractional derivative of S(t):

$${}^{C}D_{0,t}^{\alpha}S\left(t\right)=\frac{1}{\Gamma\left(1-\alpha\right)}\int_0^t\frac{\Lambda-\beta S(\tau)\frac{I(\tau)+A(\tau)}{N}-\left(\pi+\mu\right)S(\tau)+\delta P(\tau)}{(t-\tau)^{\alpha}}\,d\tau. \tag{4.5}$$

Using the modified Adams-Bashforth Scheme, the approximation becomes:

$$\begin{aligned}S_{n+2} = S_{n+1}&\\ &+\frac{3}{2}h\left(\frac{1}{h^{\alpha}}\sum_{k=0}^{n+1}w_k(\Lambda-\beta S_{n+1-k}\frac{I_{n+1-k}+A_{n+1-k}}{N}-\left(\pi+\mu\right)S_{n+1-k}+\delta P_{n+1-k})\right).\\ &-\frac{1}{2}h\left(\frac{1}{h^{\alpha}}\sum_{k=0}^{n}w_k(\Lambda-\beta S_{n-k}\frac{I_{n-k}+A_{n-k}}{N}-\left(\pi+\mu\right)S_{n-k}+\delta P_{n-k})\right)\end{aligned} \tag{4.6}$$

Simplified form of 51:

$$\begin{aligned}S_{n+2} = S_{n+1}+\frac{3}{2}\sum_{k=0}^{n+1}\frac{w_k}{h^{\alpha}}(\Lambda-\beta S_{n+1-k}\frac{I_{n+1-k}+A_{n+1-k}}{N}-\left(\pi+\mu\right)S_{n+1-k}+\delta P_{n+1-k})&\\ -\frac{1}{2}\sum_{k=0}^{n}\frac{w_k}{h^{\alpha}}(\Lambda-\beta S_{n-k}\frac{I_{n-k}+A_{n-k}}{N}-\left(\pi+\mu\right)S_{n-k}+\delta P_{n-k})&\end{aligned} \tag{4.7}$$

For each state variable, we apply the same approach

$$\begin{aligned}&S_{n+2} = S_{n+1}\\ &+\frac{3}{2}\sum_{k=0}^{n+1}\frac{w_k}{h^{\alpha}}f_S\left(t_{n+1-k},S_{n+1-k},E_{n+1-k},I_{n+1-k},A_{n+1-k},V_{n+1-k},P_{n+1-k},R_{n+1-k},W_{n+1-k}\right)\\ &-\frac{1}{2}\sum_{k=0}^{n}\frac{w_k}{h^{\alpha}}\,f_S(t_{n-k},S_{n-k},E_{n-k},I_{n-k},A_{n-k},V_{n-k},P_{n-k},R_{n-k},W_{n-k})\end{aligned}$$

$$
\begin{aligned}
&E_{n+2} = E_{n+1} \\
&+\frac{3}{2}\sum_{k=0}^{n+1}\frac{w_k}{h^\alpha} f_E\left(t_{n+1-k}, S_{n+1-k}, E_{n+1-k}, I_{n+1-k}, A_{n+1-k}, V_{n+1-k}, P_{n+1-k}, R_{n+1-k}, W_{n+1-k}\right) \\
&-\frac{1}{2}\sum_{k=0}^{n}\frac{w_k}{h^\alpha} f_E(t_{n-k}, S_{n-k}, E_{n-k}, I_{n-k}, A_{n-k}, V_{n-k}, P_{n-k}, R_{n-k}, W_{n-k}) \\
&I_{n+2} = I_{n+1} \\
&+\frac{3}{2}\sum_{k=0}^{n+1}\frac{w_k}{h^\alpha} f_I\left(t_{n+1-k}, S_{n+1-k}, E_{n+1-k}, I_{n+1-k}, A_{n+1-k}, V_{n+1-k}, P_{n+1-k}, R_{n+1-k}, W_{n+1-k}\right) \\
&-\frac{1}{2}\sum_{k=0}^{n}\frac{w_k}{h^\alpha} f_I(t_{n-k}, S_{n-k}, E_{n-k}, I_{n-k}, A_{n-k}, V_{n-k}, P_{n-k}, R_{n-k}, W_{n-k}) \\
&A_{n+2} = A_{n+1} \\
&+\frac{3}{2}\sum_{k=0}^{n+1}\frac{w_k}{h^\alpha} f_A\left(t_{n+1-k}, S_{n+1-k}, E_{n+1-k}, I_{n+1-k}, A_{n+1-k}, V_{n+1-k}, P_{n+1-k}, R_{n+1-k}, W_{n+1-k}\right) \\
&-\frac{1}{2}\sum_{k=0}^{n}\frac{w_k}{h^\alpha} f_A(t_{n-k}, S_{n-k}, E_{n-k}, I_{n-k}, A_{n-k}, V_{n-k}, P_{n-k}, R_{n-k}, W_{n-k})
\end{aligned}
\tag{4.8}
$$

$$
\begin{aligned}
&V_{n+2} = V_{n+1} \\
&+\frac{3}{2}\sum_{k=0}^{n+1}\frac{w_k}{h^\alpha} f_V\left(t_{n+1-k}, S_{n+1-k}, E_{n+1-k}, I_{n+1-k}, A_{n+1-k}, V_{n+1-k}, P_{n+1-k}, R_{n+1-k}, W_{n+1-k}\right) \\
&-\frac{1}{2}\sum_{k=0}^{n}\frac{w_k}{h^\alpha} f_V(t_{n-k}, S_{n-k}, E_{n-k}, I_{n-k}, A_{n-k}, V_{n-k}, P_{n-k}, R_{n-k}, W_{n-k}) \\
&P_{n+2} = P_{n+1} \\
&+\frac{3}{2}\sum_{k=0}^{n+1}\frac{w_k}{h^\alpha} f_P\left(t_{n+1-k}, S_{n+1-k}, E_{n+1-k}, I_{n+1-k}, A_{n+1-k}, V_{n+1-k}, P_{n+1-k}, R_{n+1-k}, W_{n+1-k}\right) \\
&-\frac{1}{2}\sum_{k=0}^{n}\frac{w_k}{h^\alpha} f_P(t_{n-k}, S_{n-k}, E_{n-k}, I_{n-k}, A_{n-k}, V_{n-k}, P_{n-k}, R_{n-k}, W_{n-k}) \\
&R_{n+2} = R_{n+1} \\
&+\frac{3}{2}\sum_{k=0}^{n+1}\frac{w_k}{h^\alpha} f_R\left(t_{n+1-k}, S_{n+1-k}, E_{n+1-k}, I_{n+1-k}, A_{n+1-k}, V_{n+1-k}, P_{n+1-k}, R_{n+1-k}, W_{n+1-k}\right) \\
&-\frac{1}{2}\sum_{k=0}^{n}\frac{w_k}{h^\alpha} f_R(t_{n-k}, S_{n-k}, E_{n-k}, I_{n-k}, A_{n-k}, V_{n-k}, P_{n-k}, R_{n-k}, W_{n-k})
\end{aligned}
$$

$$W_{n+2} = W_{n+1}$$
$$+\frac{3}{2}\sum_{k=0}^{n+1}\frac{w_k}{h^\alpha} f_W\left(t_{n+1-k}, S_{n+1-k}, E_{n+1-k}, I_{n+1-k}, A_{n+1-k}, V_{n+1-k}, P_{n+1-k}, R_{n+1-k}, W_{n+1-k}\right)$$
$$-\frac{1}{2}\sum_{k=0}^{n}\frac{w_k}{h^\alpha} f_W(t_{n-k}, S_{n-k}, E_{n-k}, I_{n-k}, A_{n-k}, V_{n-k}, P_{n-k}, R_{n-k}, W_{n-k})$$

This numerical scheme reflects the Caputo fractional derivative for the SEIAVPRW model and is designed to handle the memory effect in the fractional-order dynamics of disease spread.

5. Numerical simulation of the varicella model

This section experiments the behavior of both classical and fractional varicella model. All computations are performed using the MATLAB R2021a package on digital computer.

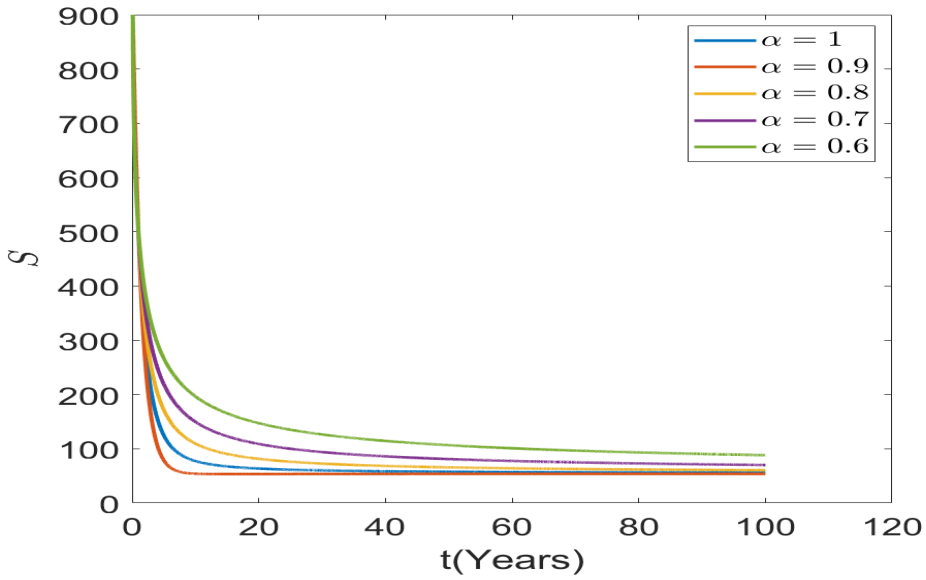

Figure 1: The dynamics of susceptible individuals (S) compartment over time, under different values of the fractional order parameter α.

Figure 1 shows the behavior of Susceptible people (S) when t is changing within the framework of different values of α. The first part of the figure characterized by a sharp decrease in the level of S corresponds to the stage of exposure, infection or vaccination of people. It can be observed how a higher order of fractional, it means that α has influence in the rate that the S decreases, and has a slow rate with a smaller steady state, while that at a small order of the fraction it gives a slow rate with a higher stead state, all these show how the history of the system exerts some influence on the present state of the epidemic and the number of remaining susceptible.

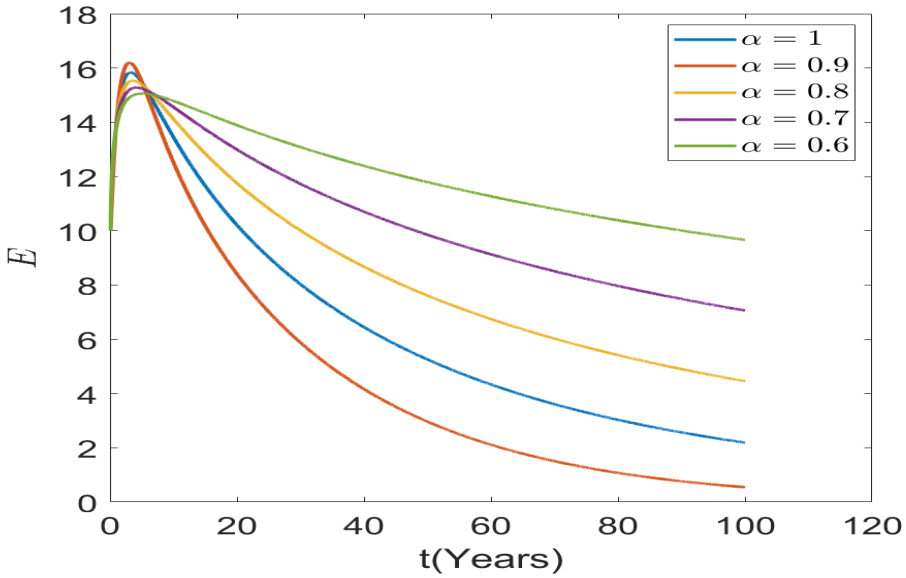

Figure 2: The dynamics of exposed individuals (E) over time for different fractional orders α.

Figure 2 depicts the trends of Exposed individuals (E) for different α values over time All trends start with an initial kink followed by a downward trend, as more exposed people become infected, asymptomatic or recoveries The rate of decline is faster for higher α and slower for lower α levels meaning more exposure period for a smaller α. This indicates that lower values of α, which capture the feature of memory effect, results in a longer period that individuals take in the exposed state before progressing to other stages in the disease progression model. The graph shows a qualitative relationship of the fractional order α on the time variation of exposed individuals in the disease model.

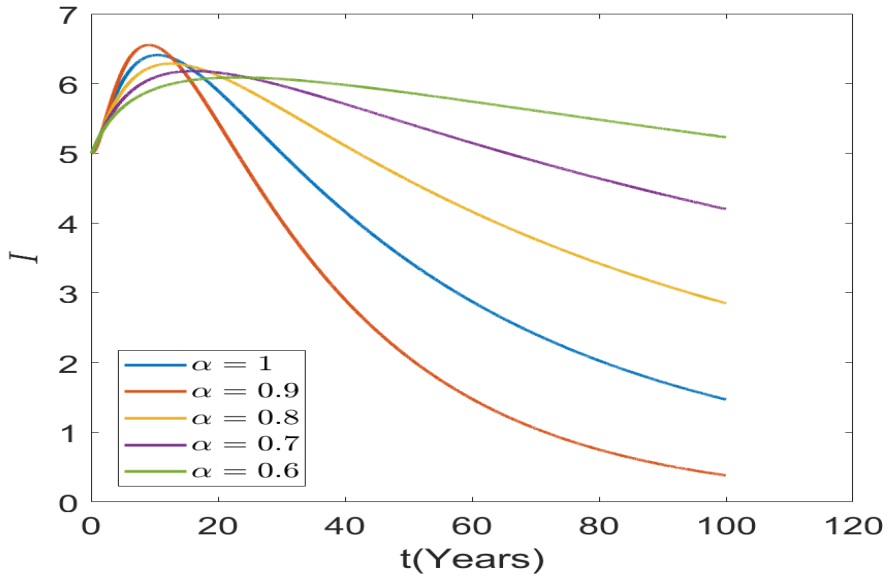

Figure 3: The dynamics of infected individuals (I) compartment over time, under different values of the fractional order parameter α.

Figure 3, the graph represents the infected population (I) against time for different α values. All curve raises initially and starts decreasing later on as infected cases starts to decrease, but the position of the peak is different with different alpha values, larger α boosts the odds earlier and larger peak while smaller α remains lower with late peak, The long-term decay of I is lower for smaller α so the epidemic tends to sustain for small α values leading to a prolonged epidemic but with a lower peak, highlighting the need for sustained interventions to control the disease spread.

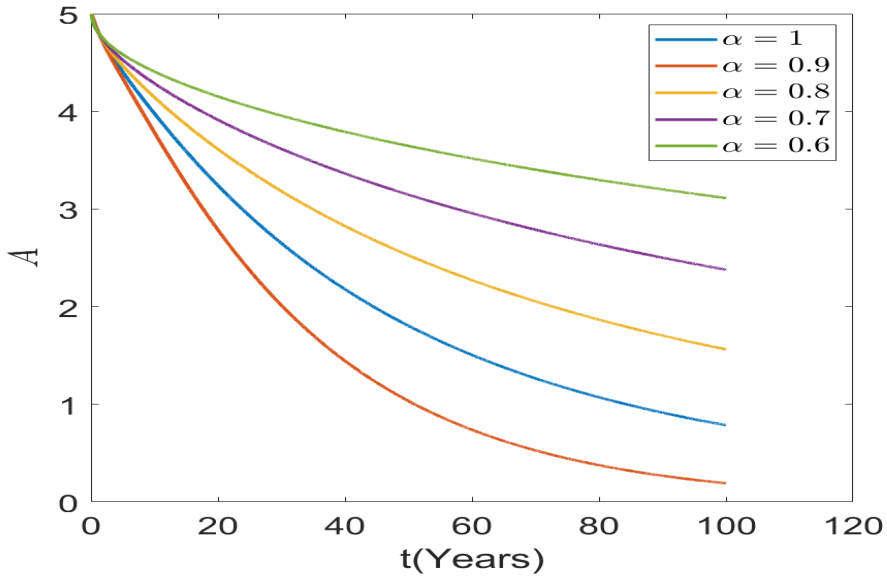

Figure 4: The dynamics of asymptomatic individuals (A) compartment over time, under different values of the fractional order parameter α.

Figure 4 illustrates the dynamics of Asymptomatic individuals (A) by time for various α. The diagrams demonstrate the decrease in A by time though the rate of such decrease is more rapid where α is greater. If α is decreasing, the decay is slower, which means that asymptomatic people are present in the population for a longer time, the stronger memory effect for small α values is pointed, where the influence of past states on the current values is stronger. Considering the analysis of the data from the graph, the higher the α values might correspond to the situations, when asymptomatic transmit faster, probably owing to effective interventions, while the lower α values might reflect the necessity of monitoring and controlling asymptomatic carriers for a longer time.

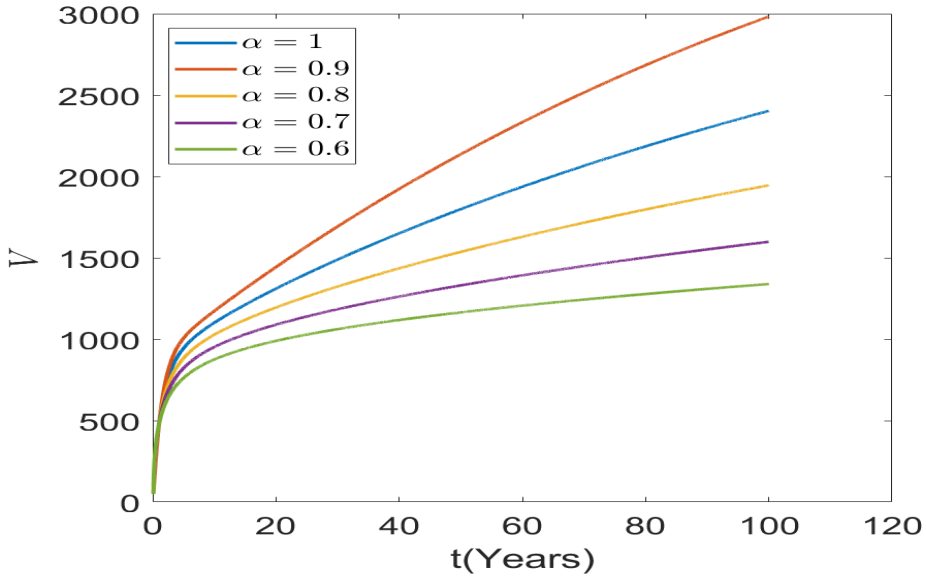

Figure 5: The dynamics of vaccinated individuals (V) compartment over time, under different values of the fractional order parameter α.

Figure 5 shows the behavior of Vaccinated transcripts in time for different α as it can be observed, the initial rate of the growing number of vaccinated individuals is expressed, and the sensitivity of this indicator to α is weak. Higher coefficient α values give a more pronounced initial upturn of the curve, whereas lesser values of α yield a relatively slower and continuous rise, suggesting a memory influence. In the long run the people getting vaccinated keep on rising but at a slower and slower rate as the curve gets closer to the maximum number of people who can be vaccinated you keep on increasing so slowly because all the vulnerable people are being vaccinated. Despite the fact there is less t cells created from the memory effect for lower α, the final number of vaccinated persons is higher, which reflects that memory effect makes it possible for the system to retain high level of vaccinated persons in the long run. This is quite evident in the use of fractional calculus in epidemiological modeling stressing on the need for historical data in vaccination and public health policies.

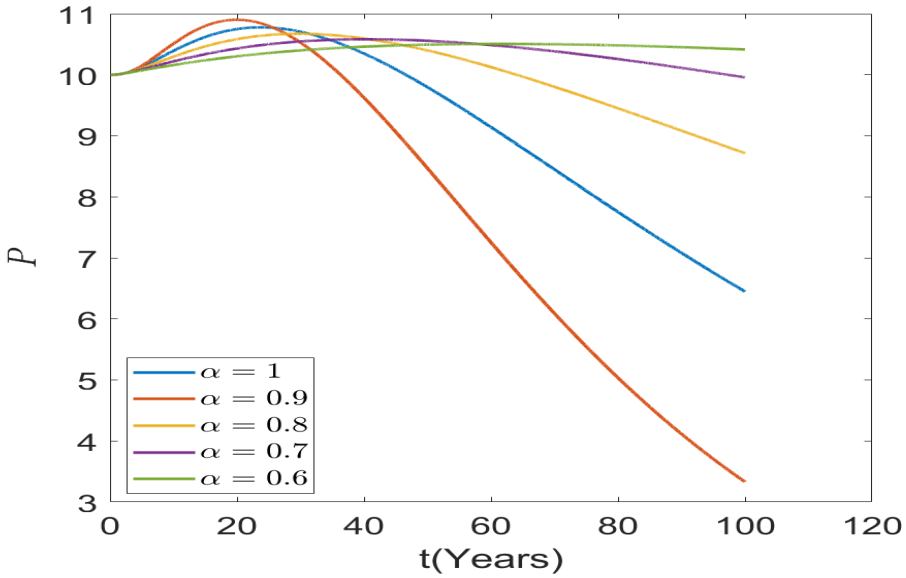

Figure 6: The dynamics of partially immune individuals (P) compartment over time, under different values of the fractional order parameter α.

(6) shows the model behaviour of the Partially Immune individuals (P) over the period of time using the numeric fractional order parameter α varying from 0.6 to 1. It depicts that with the increase of α the number of Partially Immune individuals also increase in starting phase of the model, that can be attributed with the fact that infected individuals are shifting to Partially Immune state of the model from some extent of the dynamics show the basic high rise then fall pattern but they are less steep for less steep for lower α values as the memory increases. That is, lower values of α are associated with longer persistence of partially immune people implying longer duration of the partially immune phase. This effect points up to the fact that ?fractional? should be included in analysis because it introduces a non-local characteristic that encodes the memory property in biological systems and alters the long-term dynamics of the epidemics and efficiency of health care measures.

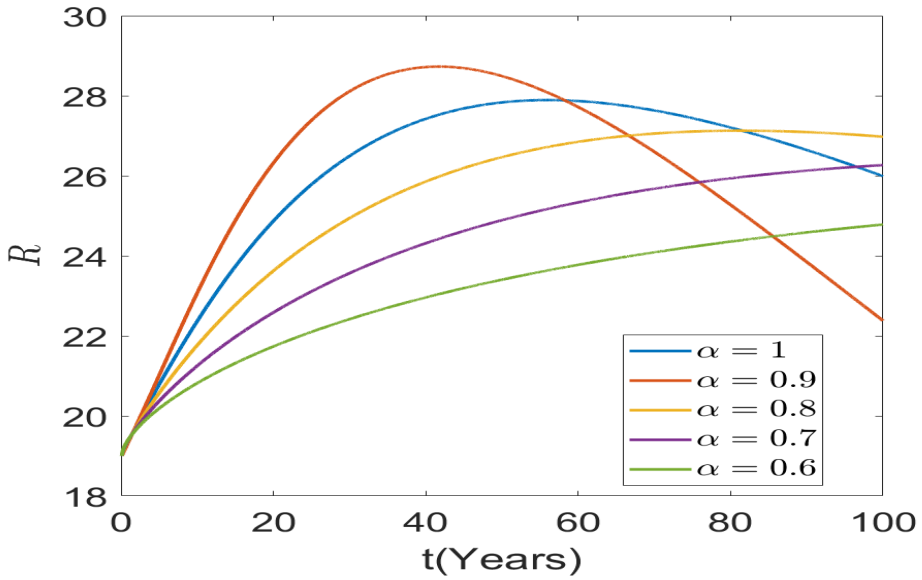

Figure 7: The dynamics of recovered individuals (R) compartment over time, under different values of the fractional order parameter α.

Figure (7), the graph illustrates the dynamics of Recovered individuals (R) against time for different α values. Higher α values make the peak to be faster and have a steep decline while lower αs show that there is a gradual decrease in the recovered population. This indicates that under stronger memory effect (lower α), individuals stay in the recovered state longer which might be due to continuous immunity or slower rate of waning immunity. The graph emphasizes the significance of fractional order when applied epidemiological models, since this has an impact on duration and dynamics of recovered population thus affecting overall disease dynamics as well as vulnerability to future outbreaks.

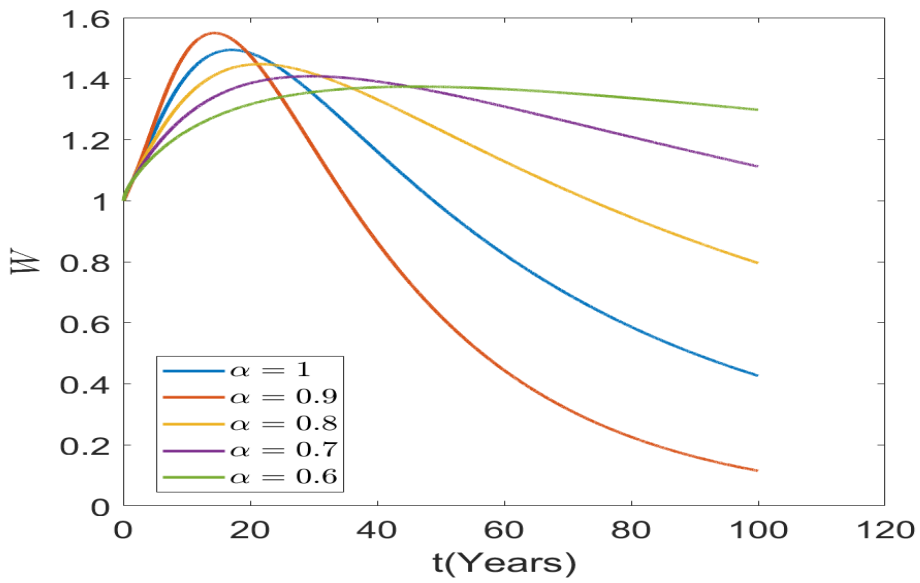

Figure 8: The dynamics of pathogen concentration in the environment (W) over time for different fractional orders, denoted by α.

Finally, Figure 8 illustrates how the Pathogen concentration in the environment (W) changes over time for different α values. All of these curves at first rise, reflecting an increasing pathogen level, as a result of infected individuals being able to release some microbial load into the populations. The peak and decay changes with α, where big α-values have an earlier peak and faster decay. Small α-values will prolong the decrease in population density because they are affected by memory effect which makes it possible for pathogen levels to remain high for long period of time. This indicates that in environments with more robust memory effects, there would be a longer-lasting presence of pathogens, which could have implications for public health strategies that seek to control environmental pathogen loads.

6. Discussion

For the dynamics of varicella transmission, a mathematical model was built through classical integer-order derivatives and later reformulated using Caputo fractional derivative to more accurately describe memory effects induced by the disease. The system was proved to be stable by convergence of equilibrium points, established by Banach Fixed-Point Theorem for existence and uniqueness. This was followed by an investigation of the local and global stability at both disease-free equilibrium points with implementation of Lyapunov functional approach. These approaches suggested that the disease-free equilibrium is globally asymptotically stable for $R_0 < 1$, and otherwise unstable indicating pathogen persistence. For discretization of the Caputo derivative, a Grunwald-Letnikov method was used. In this way, the model's ability to mirror the real-world varicella dynamic was greatly increased such as its latent infection stages and longer recovery periods. Integrating the fractional derivative could thus allow the model to consider the memory

effect, which classical models are very difficultly to reproduce. Using real-world parameter estimates, we demonstrated how behavior of the fractional-order model varied at different values of α in numerical simulations (see Figures 1-8); smaller values suppress disease spread and while a larger value enhance the disease spread.

7. Conclusion

This study utilized the Caputo fractional derivative to develop a mathematical model for varicella transmission, demonstrating that the disease's transmission rate considering both severity and age under specific contexts is effectively captured using the SEIAVPRW compartmental framework. The stability of equilibrium points was analyzed using the Lyapunov Functional Approach, while the Banach fixed-point Theorem confirmed the existence and uniqueness of solutions. The basic reproduction number R0 was identified as a critical threshold for determining whether the disease persists or dies out. Numerical simulations across different values of the fractional-order parameter α highlighted the advantages of fractional models over classical approaches. The findings suggest that incorporating Caputo fractional derivatives allows for more accurate modeling of real-world epidemiological phenomena by accounting for memory effects and historical data. This enhanced capability to reflect the progression of disease dynamics makes fractional models particularly valuable in public health. They provide high-fidelity forecasts that can better inform decision-making and control strategies compared to traditional models.

References

[1] Ahmed, E., El-Sayed, A. M. A., & El-Saka, H. A. A. (2021). On some Routh-Hurwitz conditions for fractional order systems. Mathematics, 8(4), 601.

[2] Almeida, R., Tavares, D., & Torres, D. F. (2020). Caputo fractional derivatives in epidemiology. Chaos, Solitons & Fractals, 135, 109780. https://doi.org/10.1016/j.chaos.2020.109780

[3] Atangana, A., & Baleanu, D. (2016). New fractional derivatives with non-local and non-singular kernel: Theory and application to heat transfer model. Thermal Science, 25(1), 349-356. https://doi.org/10.2298/TSCI180427186A

[4] Brown, S. T., White, C. W., & Whitley, R. J. (2021). Understanding varicella-zoster virus latency. Current Opinion in Virology, 44, 33-39.

[5] Cao, J., Sun, G. Q., & Li, X. (2020). Comparison of classical and fractional order epidemic models. Chaos, Solitons & Fractals, 134, 109704.

[6] Centers for Disease Control and Prevention. (2021). Global progress toward varicella elimination. CDC MMWR, 70(1), 1-10.

[7] Chaves, S. S., Gargiullo, P., Zhang, J. X., Civen, R., Guris, D., & Seward, J. F. (2021). The impact of varicella vaccination on varicella incidence and complications. Journal of the American Medical Association, 325(6), 532-540.

[8] Chen, W., Wu, G. C., & Yang, X. J. (2020). Fractional Calculus in Action-Applications in Physics. World Scientific Publishing.

[9] Cohen, J. I., & Brunell, P. A. (2020). Varicella-zoster virus: Biology and clinical manifestations. Journal of Infectious Diseases, 221(4), 373-382.

[10] D'Ovidio, M., Garra, R., & Polito, F. (2022). Fractional calculus and epidemiological models: A review. Mathematical Biosciences and Engineering, 19(2), 2060-2080. https://doi.org/10.3934/mbe.2022094

[11] Diethelm, K., Freed, A. D., & Luchko, Y. (2020). The solution of fractional differential equations. Fractional Calculus and Applied Analysis, 5(4), 367-402.

[12] Gershon, A. A., Takahashi, M., & Seward, J. F. (2020). Varicella vaccine in the 21st century: Optimizing protection against varicella and zoster. Pediatrics, 145(4), e20193911.

[13] Gupta, R., Raj, A., & Kumar, A. (2020). Modeling the effect of fractional order and multiple time-delays in a viral disease transmission model. Journal of Applied Mathematics and Computing, 63(1-2), 191-214.
[14] Guris, D., Jumaan, A. O., & Seward, J. F. (2020). Varicella vaccination programs: Achievements and challenges. Vaccine, 38(5), 1234-1241.
[15] Hethcote, H. W. (2020). The mathematics of infectious diseases. SIAM Review, 42(4), 599-653.
[16] Heininger, U., Seward, J. F., Jumaan, A. O., & Schmid, D. S. (2021). Complications of varicella in healthy children. Infectious Diseases Journal, 43(2), 143-148.
[17] Johnson, R. W., Alvarez-Pasquin, M. J., Bijl, M., Franco, E., & Gaillat, J. (2022). Herpes zoster epidemiology, management, and disease and economic burden in Europe. Epidemiology and Infection, 150, e1.
[18] Keeling, M. J., & Rohani, P. (2021). Modeling Infectious Diseases in Humans and Animals. Princeton University Press.
[19] Kuter, B., Matthews, H., Shinefield, H., Black, S., & Silber, J. (2021). Ten year follow-up of healthy children who received one or two injections of varicella vaccine. Pediatrics, 140(5), e20162197.
[20] Leung, J., Harpaz, R., Molinari, N. A., & Jumaan, A. O. (2020). Varicella vaccination: Clinical efficacy and impact on public health. American Journal of Public Health, 110(5), 627-633.
[21] Li, X., Cao, J., & Sun, G. Q. (2022). Impacts of fractional-order derivatives on a virus transmission model with saturated treatment function. Chaos, Solitons & Fractals, 152, 111337.
[22] Magin, R. L., McKinley, K., & Beyder, A. (2019). Fractional calculus models of complex dynamics in biological systems. Journal of Computational and Nonlinear Dynamics, 14(6), 061003.
[23] Marin, M., Guris, D., Chaves, S. S., Schmid, S., & Seward, J. F. (2020). Varicella prevention through vaccination: Impact and future perspectives. Journal of Infectious Diseases, 221(4), 583-589.
[24] Miller, E., Andrews, N., & Grant, A. (2022). Evaluating the impact of varicella vaccination in high-risk groups. Journal of Infectious Diseases, 226(2), 295-302.
[25] Sene, N. (2023). Analysis of fractional epidemic models using Caputo-Fabrizio derivative. Fractional Calculus and Applied Analysis, 26(1), 237-256. https://doi.org/10.1515/fca-2023-0011
[26] Seward, J. F., Marin, M., & Whitley, R. J. (2020). Management of varicella in high-risk populations. Clinical Microbiology Reviews, 33(4), e00074-19.
[27] Smith, K. M., Brown, L. P., & Davis, M. E. (2021). Pathophysiology of varicella-zoster virus latency and reactivation. Virology Journal, 18(1), 1-15.
[28] Sun, H., Zhang, Y., Baleanu, D., Chen, W., & Chen, Y. (2019). A new collection of real world applications of fractional calculus in science and engineering. Communications in Nonlinear Science and Numerical Simulation, 64, 213-231.
[29] Whitley, R. J., Haines, H., & Jackson, M. (2021). Antiviral treatments for varicella-zoster virus infections. New England Journal of Medicine, 384(1), 36-45.
[30] World Health Organization. (2019). Global epidemiology and burden of varicella. WHO Bulletin, 97(9), 625-632.
[31] Yang, X. J., & Liu, H. J. (2021). Fractional derivatives in epidemiological models. Chaos, Solitons & Fractals, 144, 110667.
[32] Eiman, Shah, K., Sarwar M., Abdeljawad T. On mathematical model of infectious disease by using fractals fractional analysis. Discrete and Continuous Dynamical Systems-S, 17 (2024) 3064-3085. Doi: 10.3934/dcdss.2024073
[33] Shah, K., Sher M., Sarwar M., Abdeljawad T. Analysis of a nonlinear problem involving discrete and proportional delay with application to Houseflies model. AIMS Mathematics, 9 (2024) 7321-7339. doi: 10.3934/math.2024355
[34] Shah, K., Nas H., Abdeljawad T., Abdalla B. Study of fractional order dynamical system of viral infection disease under piecewise derivative. CMES-Computer Modeling in Engineering & Sciences, 136 (2023) 921-941.